nature portfolio

https://doi.org/10.1038/s41551-022-00925-y

Supplementary information

Unbiased discovery of autoantibodies associated with severe COVID-19 via genome-scale self-assembled DNA-barcoded protein libraries

In the format provided by the authors and unedited

Contents

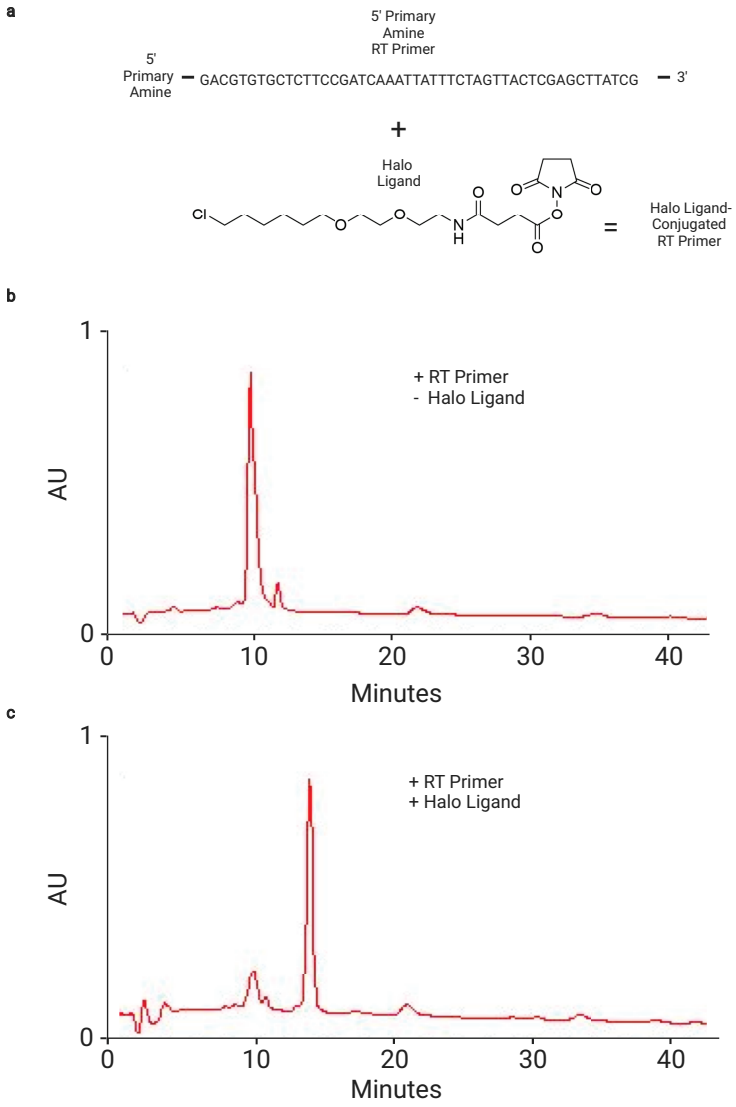

Supplementary Fig. 1: HaloLigand conjugation to the reverse transcription primer. a, Above is the oligonucleotide reverse transcription (RT) primer sequence modified with a 5' primary amine. Below is the HaloLigand with a reactive succinimidyl ester group, separated by one ethylene glycol moiety (O2). The succinimidyl ester reacts with the primary amine to form an amide-bond between the RT primer and the HaloLigand, resulting in the HaloLigand-conjugated RT primer. **b**, HPLC chromatogram of the RT primer without the HaloLigand modification. **c**, HPLC chromatogram of the RT primer with the HaloLigand modification after purification. The conjugated product elutes later due to increased hydrophobicity conferred by the modification.

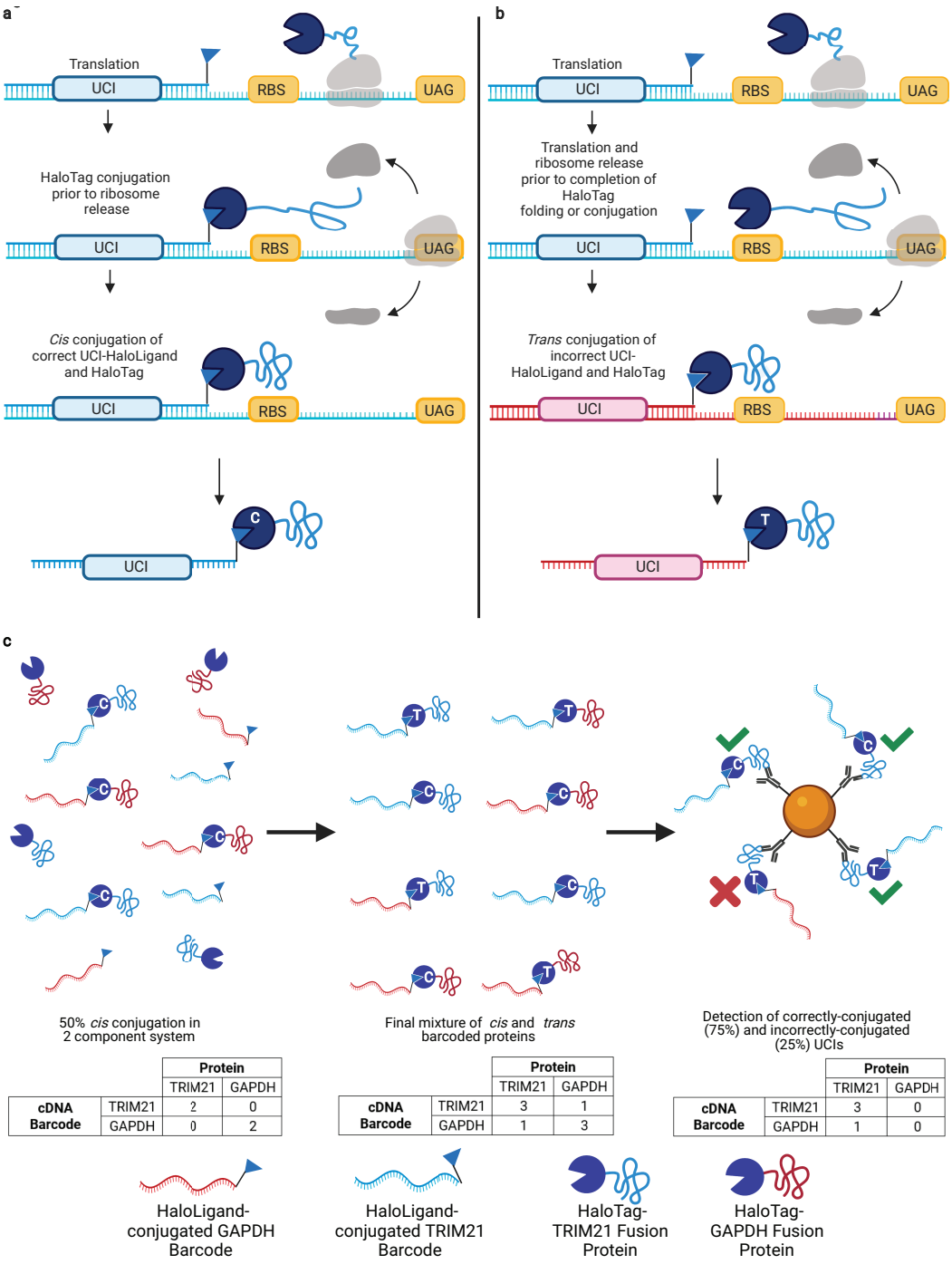

		Protein	
		TRIM21	GAPDH
cDNA Barcode	TRIM21	2	0
	GAPDH	0	2

		Protein	
		TRIM21	GAPDH
cDNA Barcode	TRIM21	3	1
	GAPDH	1	3

		Protein	
		TRIM21	GAPDH
cDNA Barcode	TRIM21	3	0
	GAPDH	1	0

Supplementary Fig. 2: *Cis* versus *trans* UCI-ORF associations. Schematic of *cis* product **a**, versus *trans* side product **b**, UCI-ORF conjugation during translation of a MIPSA IVT-RNA library. **c**, Left panel: 50% *cis* conjugates ("C") composed of the correct protein-UCI associations (e.g. blue UCI with blue protein). Middle panel: unconjugated proteins then randomly associates with unconjugated UCIs in *trans* ("T"). Right panel: the ratio of correctly to incorrectly IPed UCIs in this two-species experiment is 3:1 (75%:25%), similar to experimental observations (**Fig. 2a**).

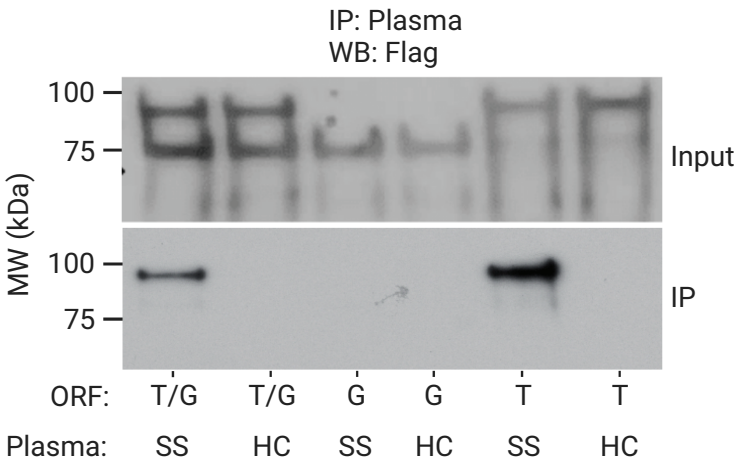

Supplementary Fig. 3: Two-plex translation and IP of TRIM21 and GAPDH. *TRIM21* (T) and *GAPDH* (G) IVT-RNA-cDNA were translated either separately or together and then subjected to IP with healthy control (HC) or Sjogren's Syndrome (SS) plasma. Analysis was by immunoblotting with the M2 antibody that recognizes the common FLAG epitope tag included in linker between the HaloTag and the protein.

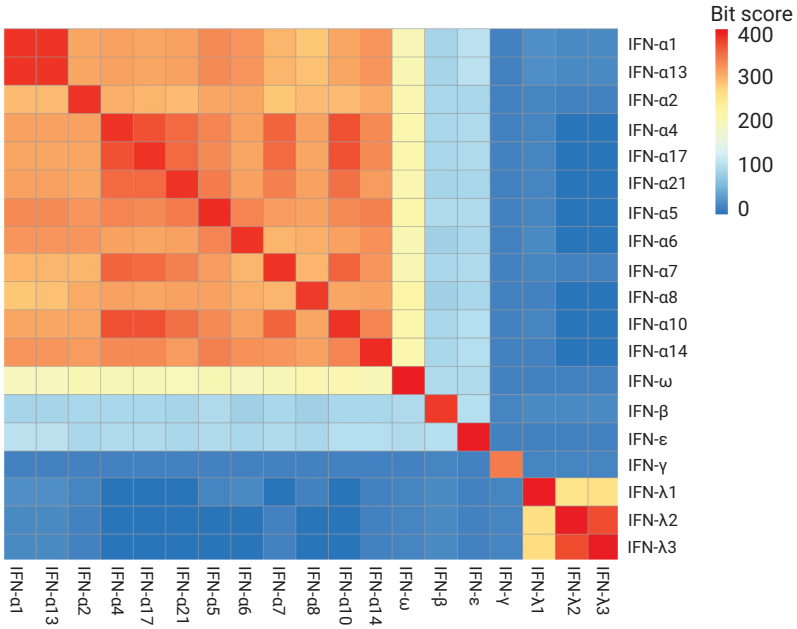

Supplementary Fig. 4: Sequence homology of interferons. Pairwise blastp alignment bitscore matrix for all interferon (IFN) proteins shown in **Fig. 5d**.

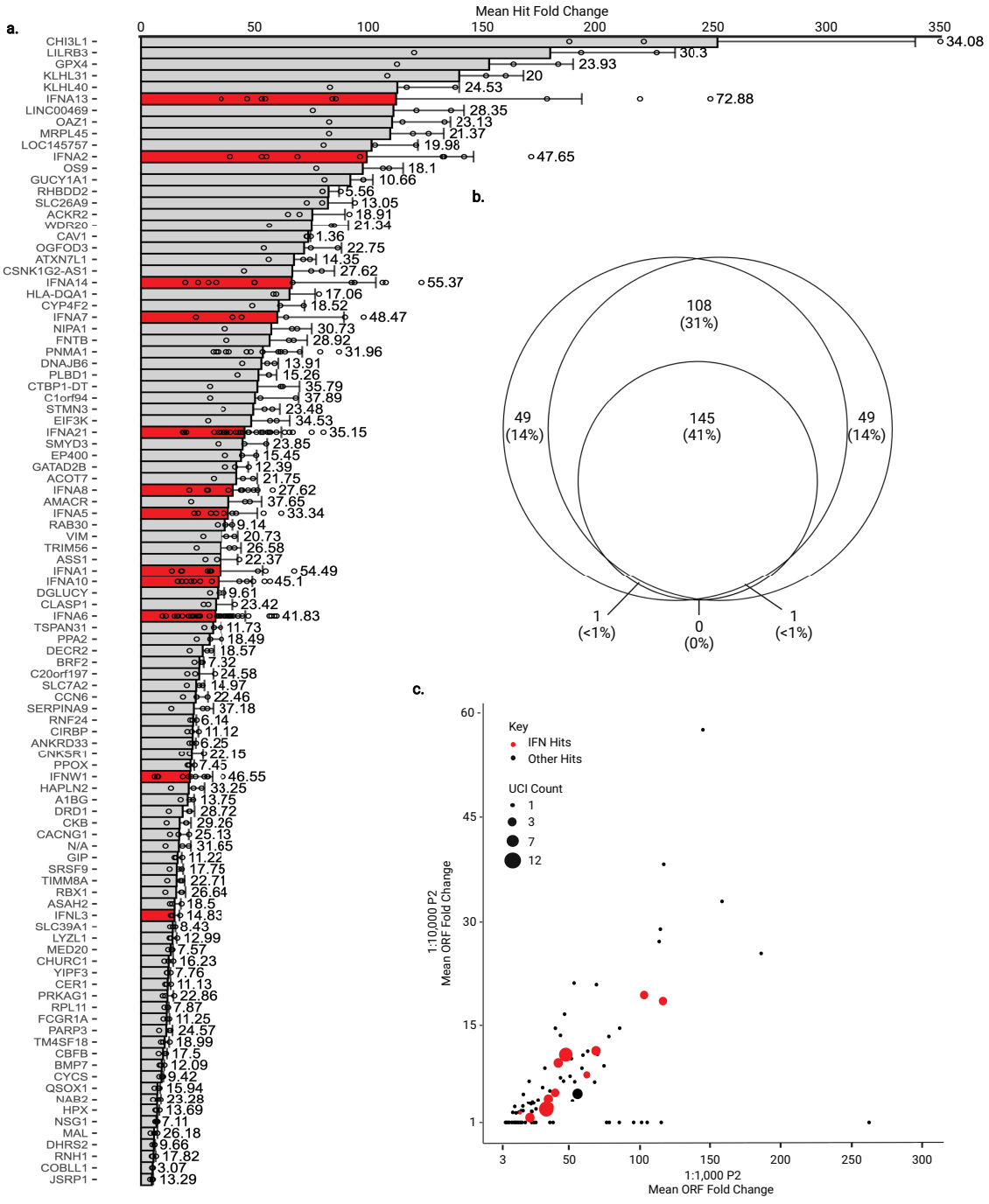

Supplementary Fig. 5: Reproducibility and linearity of MIPSA detection of patient P2's autoantibodies. a, Mean and standard deviation of the 100 ORF fold changes for all consistently reactive monospecific UCIs (fold change > 3 in all 3 replicates). The values to the right of the error bars are the coefficients of variation. **b**, Numbers of overlapping reactive monospecific UCIs over three independent MIPSA analyses of P2 plasma. Areas are proportional to numbers of hits. **c**, Mean ORF fold changes for P2 plasma, compared to P2 plasma diluted 10-fold into a background of a healthy control plasma. Dot sizes depict the numbers of reactive UCIs corresponding to each ORF.

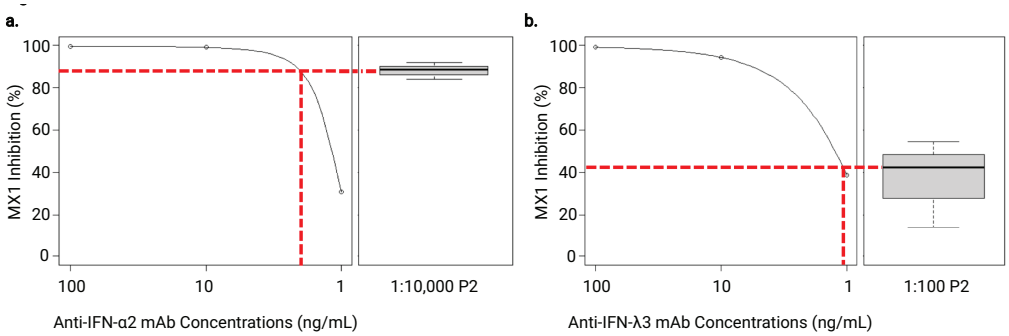

Supplementary Fig. 6: Titration-based estimate of patient P2's interferon autoantibody levels. Mouse monoclonal blocking antibodies were used at different concentrations in the cell-based IFN neutralization assay: **a**, IFN-α2 and **b**, IFN-λ3. Neutralization curves were fit and used to estimate patient P2's corresponding interferon autoantibody levels. The plasma dilutions shown were selected to be within the dynamic range of the assay; neutralizing activity of P2 plasma at the dilution shown was assayed in technical triplicate. For the 1:10,000 P2 IFN-α2 neutralization test, the median +/- standard deviation of the percent inhibition of *MX1* induction is 88.69 +/-3.24, respectively. For the 1:100 P2 IFN-λ3 neutralization test, the median +/- standard deviation of the percent inhibition of *MX1* induction is 42.58 +/-17.16, respectively.

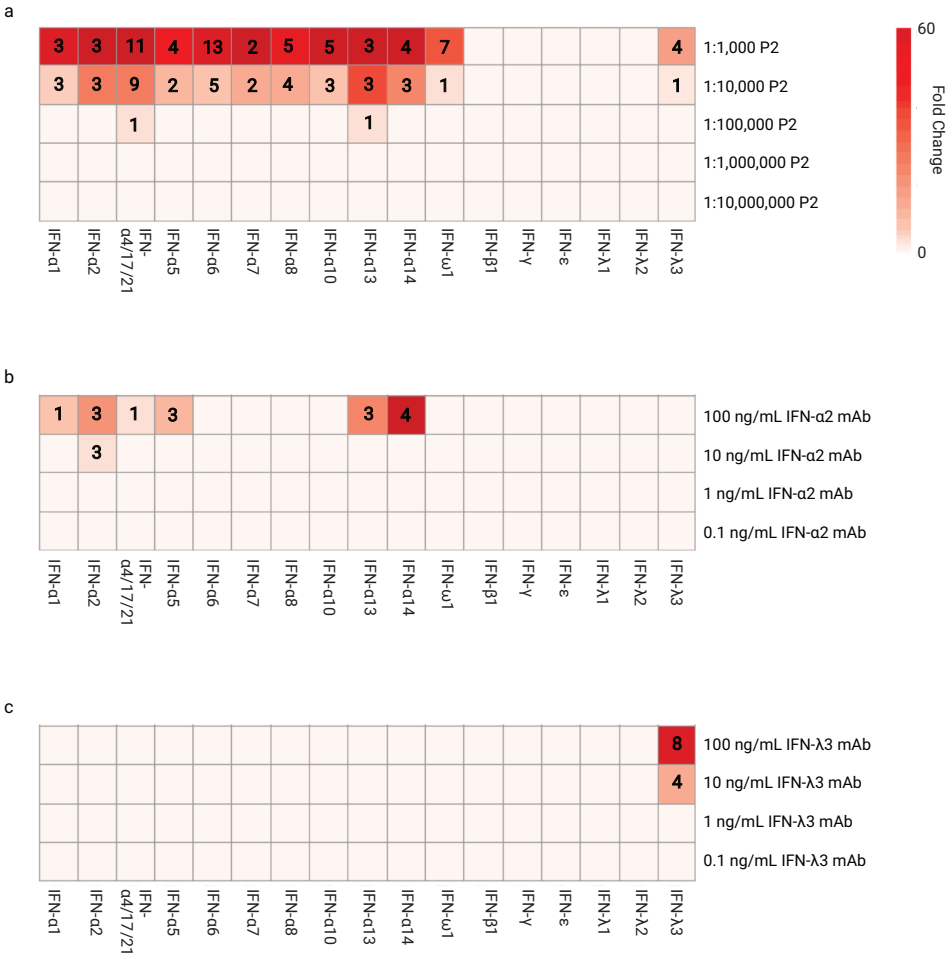

Supplementary Fig. 7: MIPSA analysis of interferon antibodies in serial dilution. Summary of interferon reactivity detected by MIPSA in serially diluted P2 plasma (**a**), IFN-α2 mAb (**b**), and IFN-λ3 mAb (**c**). Hits fold-change values (color of cell) and the number of reactive UCIs (number in cell) are provided as in **Fig. 5d**.

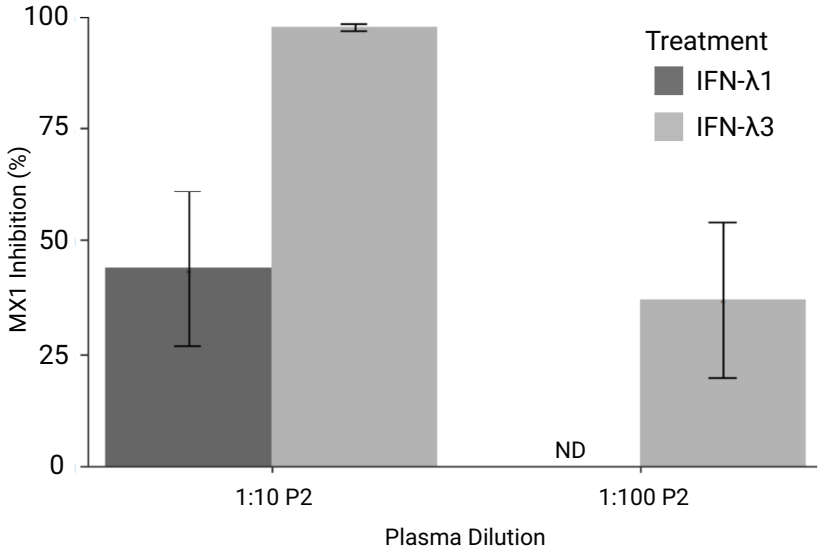

Supplementary Fig. 8: IFN-λ3 autoantibodies do not efficiently neutralize IFN-λ1. The IFN-λ3 neutralizing activity of patient P2's plasma was compared to its IFN-λ1 neutralizing activity. Neutralization of IFN-λ3 was complete and partial at 1:10 and 1:100 dilutions, respectively. Neutralization of IFN-λ1 was partial and not detected at 1:10 and 1:100 dilutions, respectively. Mean +/- standard deviation of percent inhibition of MX1 induction by IFN-λ3 were 97.02 +/-0.77 for 1:10 P2 and 36.94 +/-17.16 for 1:100 P2. Mean +/- standard deviation of percent inhibition of MX1 induction by IFN-λ1 were 43.81 +/-17.07 for 1:10 P2 and 0 (not detected) for 1:100 P2.

Study Population							
Group		#	Age	Sex	Black	White	Other
Severe COVID-19	Died	17	67 (27,87)	F: 8, M: 9	9	4	4
	Ventilated	13	67 (27,82)	F: 9, M: 4	4	4	5
	Got O2	22	52 (27,82)	F: 9, M: 13	8	8	6
	No O2	3	46 (22,49)	F: 0, M: 3	0	3	0
COVID-19 Controls	Mild/Mod	10	35 (19,55)	F: 6, M: 4	0	8	2
	Healthy Control	10	41.5 (22,66)	F: 3, M: 7	3	5	2
Myositis	Inclusion Body	10	53.9 (43.6,60.6)	F: 7, M: 3	1	7	2
	Healthy Control	10	36.5 (20,60)	F: 5, M: 5	2	8	0

Supplementary Table 1: Severe COVID-19 patients and control study participants. Individuals' ages were provided to investigators as intervals to protect identities of study participants.

Symbol	Gene_name	AAgAtlas	#Severe	#Controls	#Reactive_UCIs	hits_FCs	Cluster_ID
ASTL	astacin like metalloendopeptidase	no	2	1	2	5.7, (3.8,7.5)	1
BEND7	BEN domain containing 7	no	6	1	7	5.5, (3.2,16.1)	2
BLVRA	biliverdin reductase A	no	1	0	3	17.9, (17.9,17.9)	1
BMPR2	bone morphogenetic protein receptor type 2	yes	3	0	2	3.5, (3.2,4.0)	1
C1orf94	chromosome 1 open reading frame 94	no	12	0	8	5.2, (3.0,15.4)	3
C3orf18	chromosome 3 open reading frame 18	no	1	0	2	3.3, (3.3,3.3)	1
CALHM1	calcium homeostasis modulator 1	no	3	1	2	3.9, (3.3,4.4)	1
CAV2	caveolin 2	no	9	0	2	3.7, (3.1,5.0)	4
CCDC106	coiled-coil domain containing 106	no	4	0	10	4.4, (3.1,7.2)	2
CCDC146	coiled-coil domain containing 146	no	5	0	3	3.6, (3.1,4.7)	1
CD2BP2	CD2 cytoplasmic tail binding protein 2	no	2	0	3	14.9, (5.1,24.8)	5
CDC73	cell division cycle 73	no	1	0	2	4.1, (4.1,4.1)	1
CHMP7	charged multivesicular body protein 7	no	10	1	3	3.6, (3.1,4.7)	4
CTAG2	cancer/testis antigen 2	no	3	0	6	5.2, (3.0,9.4)	1
CYP2S1	cytochrome P450 family 2 subfamily S member 1	no	2	0	3	4.1, (3.2,5.0)	1
DNAJC17	DnaJ heat shock protein family (Hsp40) member C17	no	4	0	2	3.2, (3.0,3.6)	2
DOLPP1	dolichyldiphosphatase 1	no	3	0	3	4.7, (3.9,5.1)	1
EHD1	EH domain containing 1	no	2	0	14	33.4, (3.6,63.2)	1
EHD2	EH domain containing 2	no	2	0	4	4.3, (3.0,5.6)	1
ELOA2	elongin A2	no	9	0	2	3.5, (3.0,4.9)	4
EXD1	exonuclease 3'-5' domain containing 1	no	1	0	2	7.2, (7.2,7.2)	5
EXOC4	exocyst complex component 4	no	17	0	7	3.9, (3.0,4.9)	4
FAM185A	family with sequence similarity 185 member A	no	4	1	2	3.4, (3.2,3.6)	1
FAM32A	family with sequence similarity 32 member A	no	4	0	2	3.6, (3.2,4.0)	2
FBXL19	F-box and leucine rich repeat protein 19	no	2	0	3	7.0, (3.0,11.0)	1
FDFT1	farnesyl-diphosphate farnesyltransferase 1	no	1	0	2	46.8, (46.8,46.8)	1
FRG1	FSHD region gene 1	no	5	0	3	3.6, (3.2,4.3)	1
FUT9	fucosyltransferase 9	no	2	1	3	3.9, (3.5,4.3)	1
GATA2	GATA binding protein 2	no	5	0	2	3.6, (3.0,4.3)	4
GIMAP8	GTPase, IMAP family member 8	no	1	0	2	4.7, (4.7,4.7)	1
HNF4A	hepatocyte nuclear factor 4 alpha	no	1	0	2	11.7, (11.7,11.7)	1
HNRNPUL1	heterogeneous nuclear ribonucleoprotein U like 1	no	3	0	4	5.7, (3.6,8.6)	1
HPGD	15-hydroxyprostaglandin dehydrogenase	no	1	0	4	6.0, (6.0,6.0)	1
IFNA10	interferon alpha 10	no	2	0	5	18.8, (16.8,20.7)	2
IFNA13	interferon alpha 13	no	4	0	2	22.5, (4.6,51.4)	2
IFNA14	interferon alpha 14	no	3	0	2	19.3, (3.2,44.2)	2
IFNA2	interferon alpha 2	yes	2	0	3	42.5, (25.2,59.8)	2
IFNA21	interferon alpha 21	no	2	0	10	25.1, (14.9,35.3)	2
IFNA5	interferon alpha 5	no	2	0	3	14.6, (14.6,14.7)	2
IFNA6	interferon alpha 6	no	4	1	12	9.4, (3.3,21.8)	2
IFNA8	interferon alpha 8	no	7	0	5	9.7, (3.1,36.4)	2
IFNL3	interferon lambda 3	no	3	1	5	5.5, (4.2,7.6)	1
IFNW1	interferon omega 1	no	2	0	5	29.6, (10.6,48.5)	2
IKZF3	IKAROS family zinc finger 3	no	2	0	4	13.8, (3.3,24.2)	1
KCNJ12	potassium inwardly rectifying channel subfamily J member 12	no	1	0	2	3.1, (3.1,3.1)	1
KCNJ14	potassium inwardly rectifying channel subfamily J member 14	no	2	0	3	3.9, (3.2,4.6)	1
KLHL31	kelch like family member 31	no	1	0	2	11.3, (11.3,11.3)	2
KLHL40	kelch like family member 40	no	1	0	4	8.4, (8.4,8.4)	2
LALBA	lactalbumin alpha	no	1	0	2	3.9, (3.9,3.9)	1
LINC01547	long intergenic non-protein coding RNA 1547	no	2	0	6	19.3, (3.4,35.1)	1
MAGEE1	MAGE family member E1	no	1	0	3	17.9, (17.9,17.9)	1

Supplementary Table 2: Proteins reactive in severe COVID-19 patients. Symbol, gene symbol; AAgAtlas, is protein listed in AAgAtlas 1.0?; #Severe, number of severe COVID-19 patients with reactivity to at least one UCI; #Controls, number of control donors (healthy or mild-moderate COVID-19) with reactivity to at least one UCI; #Reactive_UCIs, number of reactive UCIs associated with given ORF; Hits_FCs, mean and range (minimum to maximum) of per-ORF maximum hits fold-change observed among the patients with the reactivity; Cluster_ID, antigen cluster defined by **Fig 4b**.

Symbol	Gene_name	AAgAtlas	#Severe	#Controls	#Reactive_UCIs	hits_FCs	Cluster_ID
MAX	MYC associated factor X	no	7	0	10	13.0, (3.1,30.9)	3
MBD3L1	methyl-CpG binding domain protein 3 like 1	no	2	0	5	8.1, (4.1,12.2)	1
MKX	mohawk homeobox	no	6	1	3	3.8, (3.1,4.8)	4
MPPED2	metallophosphoesterase domain containing 2	no	5	0	3	5.2, (3.1,11.7)	1
NACC1	nucleus accumbens associated 1	no	2	0	12	74.9, (74.7,75.2)	5
NAPSA	napsin A aspartic peptidase	no	3	1	3	4.1, (3.1,4.7)	1
NBPF1	NBPF member 1	no	1	0	2	6.9, (6.9,6.9)	1
NBPF15	NBPF member 15	no	1	0	2	3.5, (3.5,3.5)	1
NOXO1	NADPH oxidase organizer 1	no	3	0	6	3.9, (3.0,4.8)	1
NT5C1A	5'-nucleotidase, cytosolic IA	no	3	1	2	26.9, (7.2,59.9)	5
NUP62	nucleoporin 62	no	1	0	7	8.4, (8.4,8.4)	1
NVL	nuclear VCP like	no	1	0	2	21.6, (21.6,21.6)	1
OLFM4	olfactomedin 4	yes	5	1	3	12.9, (4.4,29.8)	5
PIMREG	PICALM interacting mitotic regulator	no	4	1	4	3.8, (3.5,4.1)	1
PLEKHF1	pleckstrin homology and FYVE domain containing 1	no	2	0	3	3.3, (3.1,3.5)	1
PML	PML nuclear body scaffold	no	1	0	4	29.7, (29.7,29.7)	1
PNMA1	PNMA family member 1	yes	1	0	3	6.4, (6.4,6.4)	2
PNMA5	PNMA family member 5	no	2	0	5	5.7, (4.0,7.4)	2
POLDIP3	DNA polymerase delta interacting protein 3	no	5	0	3	3.3, (3.1,3.7)	4
POMP	proteasome maturation protein	no	1	0	2	3.2, (3.2,3.2)	1
POU6F1	POU class 6 homeobox 1	no	1	0	3	12.0, (12.0,12.0)	1
PQBP1	polyglutamine binding protein 1	no	5	0	2	3.2, (3.0,3.5)	5
PRKAR2B	protein kinase cAMP-dependent type II regulatory subunit beta	no	1	0	3	7.3, (7.3,7.3)	1
PXDNL	peroxidasin like	no	4	0	4	3.5, (3.1,3.9)	2
RBM17	RNA binding motif protein 17	no	1	0	3	23.6, (23.6,23.6)	1
RCAN3	RCAN family member 3	no	1	0	5	5.3, (5.3,5.3)	1
RPL13AP3	ribosomal protein L13a pseudogene 3	no	4	1	5	3.4, (3.1,3.7)	1
RPL15	ribosomal protein L15	no	11	1	6	3.4, (3.1,3.9)	3
RPP14	ribonuclease P/MRP subunit p14	no	1	0	6	35.9, (35.9,35.9)	1
RPP30	ribonuclease P/MRP subunit p30	no	1	0	4	46.1, (46.1,46.1)	1
RUFY4	RUN and FYVE domain containing 4	no	1	0	4	16.3, (16.3,16.3)	1
SNRPA1	small nuclear ribonucleoprotein polypeptide A'	no	1	0	2	5.3, (5.3,5.3)	1
SPEF1	sperm flagellar 1	no	2	0	5	5.9, (3.2,8.5)	1
SPRR1B	small proline rich protein 1B	no	1	0	4	7.5, (7.5,7.5)	1
SSNA1	SS nuclear autoantigen 1	yes	1	0	5	12.2, (12.2,12.2)	2
STPG3	sperm-tail PG-rich repeat containing 3	no	1	0	2	3.6, (3.6,3.6)	1
SYT2	synaptotagmin 2	no	6	1	4	3.6, (3.2,4.5)	5
TBC1D10B	TBC1 domain family member 10B	no	3	1	2	3.4, (3.1,4.1)	1
TFAP4	transcription factor AP-4	no	1	0	5	3.7, (3.7,3.7)	1
TMPO	thymopoietin	no	2	0	5	15.7, (3.7,27.7)	1
TNFSF14	TNF superfamily member 14	no	1	0	2	3.7, (3.7,3.7)	1
TOX4	TOX high mobility group box family member 4	no	1	0	3	9.9, (9.9,9.9)	1
TRAIP	TRAF interacting protein	no	2	0	3	4.7, (3.4,6.0)	1
VAV1	vav guanine nucleotide exchange factor 1	no	1	0	4	10.2, (10.2,10.2)	1
ZBTB18	zinc finger and BTB domain containing 18	no	1	0	2	3.3, (3.3,3.3)	1
ZFP2	ZFP2 zinc finger protein	no	2	1	3	4.9, (3.1,6.7)	1
ZMAT2	zinc finger matrin-type 2	no	6	0	5	3.6, (3.1,4.1)	2
ZNF146	zinc finger protein 146	no	2	0	8	16.4, (3.1,29.7)	1
ZNF232	zinc finger protein 232	no	2	1	4	4.6, (3.5,5.8)	1
ZNF678	zinc finger protein 678	no	3	1	2	6.6, (3.4,12.8)	1
ZSCAN32	zinc finger and SCAN domain containing 32	no	1	0	2	11.3, (11.3,11.3)	1
ZSCAN5A	zinc finger and SCAN domain containing 5A	no	3	0	4	4.0, (3.2,5.3)	1

Supplementary Table 2. (continued)

Names	Sequences
T7-Pep2_PCR1_F	5’-ATAAAGGTGAGGGTAATGTC-3'
Nextera Index 1	5’-CAAGCAGAAGACGGCATACGAGAT[i7]GTCTCGTGGGCTCGG-3'
PhIP_PCR2_F	5’-AATGATACGGCGACCACCGAGATCTACAC-**[i5]-**GGAGCTGTCGTATTCCAGTC-3'
P7.2	5’-CAAGCAGAAGACGGCATACGA-3'
T7-Pep2_PCR1_R+ad_min	5’-CTGGAGTTCAGACGTGTGCTCTTCCGATCAGTTACTCGAGCTTATCGT-3'
PhIP_PCR2_R	5'-CAAGCAGAAGACGGCATACGAGAT-**[i7]-**GTGACTGGAGTTCAGACGTGTGCTC-3'
T7-Pep2.2_SP_subA	5’-CTCGGGGATCCAGGAATTCCGCTGCGT-3'
MISEQ_MIPSA_R2	5’- ATGACGACAAGCCATGGTCGAATCAAACAAGTTTGTACAAAAAAGTTGGC-3'
MIPSA_i5_NextSeq_SP	5’-GGATCCCCGAGACTGGAATACGACAGCTCC-3'
Standard_i7_SP	5’-GATCGGAAGAGCACACGTCTGAACTCCAGTCAC-3'
HL-32_ad	HL-GACGTGTGCTCTTCCGATCAAATTATTTCTAGGTACTCGAGCTTATCG-3'
MX1_Forward	5’-ACCACAGAGGCTCTCAGCAT-3'
MX1_Reverse	5’-CTCAGCTGGTCCTGGATCTC-3'
GAPDH_Forward	5’-GAGTCAACGGATTTGGTCGT-3'
GAPDH_Reverse	5’-TTGATTTTGGAGGGATCTCG-3'
BT2_F	5’-GTCAGAGTGACACACTGT-3'
BT2_R	5’-AGAGTGACAGTCACAGTG-3'
BG4_F	5’-CACTGACTGTGTGAGTGT-3'
BG4_R	5’-TGAGACACAGTGAGTCAC-3'
NT5C1A_F	5’-CTCACAGACAGACGTCA-3'
NT5C1A_R	5’-TGTCAGTCAGTGAGTGTG-3'

Supplementary Table 3: Primer sequences used in this study.

Supplementary Data File 1: Hits fold-change MIPSA data matrix for UCIs of reactive proteins in severe COVID-19 patients. Proteins were included if they had at least two reactive UCIs in at least one severe patient and were not reactive in more than one control (healthy or mild/moderate convalescent plasma). Proteins were not included if they were reactive in a single severe patient and a single control. Each row corresponds to a single UCI, organized by protein in alphabetical order (gene symbol provided to left of underscore). Each column is an individual COVID-19 patient. If the UCI read counts were not significantly enriched versus the mock IPs, it is reported as "1". If the UCI read counts were significantly enriched versus mock IPs, the fold-change estimate (from EdgeR) is provided.

Source Data 1: Unprocessed western blot of Figure 1E.

Source Data 2: Unprocessed western blot of top panel in Figure 1F.

Source Data 3: Unprocessed western blot of middle panel in Figure 1F.

Source Data 4: Unprocessed western blot of bottom panel in Figure 1F.

Source Data 5: Unprocessed western blot of top panel in Figure S3.

Source Data 6: Unprocessed western blot of bottom panel in Figure S3.